A Benchmark Construction of Positron Crystal Undulator

V.V. Tikhomirov

Research Institute for Nuclear Problems, Bobruiskaya str., 11, 220050, Minsk, Belarus

Abstract

Optimization of a positron crystal undulator (CU) is addressed. The ways to assure both the maximum intensity and minimum spectral width of positron CU radiation are outlined. We claim that the minimum CU spectrum width of 3 – 4% is reached at the positron energies of a few GeV and that the optimal bending radius of crystals planes in CU ranges from 3 to 5 critical bending radii for channeled particles. Following suggested approach a benchmark positron CU construction is devised and its functioning is illustrated using the simulation method widely tested by experimental data.

Key words: channeling, crystal undulator, x-rays, gamma-rays, channeling radiation, undulator radiation.

Email address: vvtikh@mail.ru (V.V. Tikhomirov).

1 Introduction

Crystal undulators (CUs) [1,2] open up wide possibilities for designing sources of intense x- and γ-radiation. The unique properties of CUs are assured by both the intra-atomic strength and the inter-atomic space scale of the field of crystal planes. After the modulation of transverse displacament of crystal planes in CUs their field allows to induce the undulator-like motion of channeled particles characterized by the record-breaking acceleration and oscillation frequency. These unique properties open up a way to generate intense hard narrow-spectrum radiation using particle beams of reasonable energies.

Though CUs were proposed quite long ago [1,2], reliable realistic description of their functioning has become possible only after the development [3,4] and experimental validation [5,6] of the corresponding simulation tool.

Both various approaches to CU fabrication and different views on the previous achievements in CU studies have been addressed in [4,7,8]. Our analysis [4] of both conducted and suggested experiments demonstrates limited perspectives of electron CUs and stimulates more active investigation of the positron case. In this paper we address the problem of finding an optimal construction of positron CU suggesting the ways how to increase the intensity and reduce the spectral width of the CU radiation.

A method of optimal positron CU parameter search is outlined in Section 2. Some details of our simulation method are discussed in Section 3 along with the results of its applications to both the recent test [9] of the short-period electron CU [10] and 6.7 GeV channeling positron radiation experiment [11]. Section 4 describes some benchmark positron CU configuration and illustrates

its functioning.

2 CU parameter choice

In order both to describe the necessary features of the positron CUs and to devise a method to fix their parameters we will consider the positron motion and radiation in the field of crystal planes transversely modulated according to the function

$$X(z) = A\cos\left(\frac{2\pi}{\lambda_U}z\right) = A\cos(k_z z), \quad k_z = \frac{2\pi}{\lambda_U}, \tag{1}$$

where A and λ_U are CU amplitude and period respectively, x axis is normal and z axis is parallel to the crystal planes before modulation.

The positron transverse coordinate $x(z) + X(z)$ measured in the laboratory reference frame obeys relativistic Lorentz equation of motion in the electric field of the modulated planes (1). This equation can be transformed to that for the positron coordinate $x(z)$ measured from some modulated crystal plane and governed by the effective planar potential $V_{eff}[x, R(z)]$ (see Fig. 1), depending on the local crystal bending radius

$$R(z) \approx \left(\frac{d^2X(z)}{dz^2}\right)^{-1} = -\frac{1}{\cos(k_z z)\ A\,k_z^2}, \tag{2}$$

having the minimum absolute value

$$R_{\min} = 1/Ak_z^2. \tag{3}$$

In principle, since the bending radius (2) depends on z, the particle transverse motion in the effective potential is accompanied by the transverse energy $\varepsilon_\perp =$

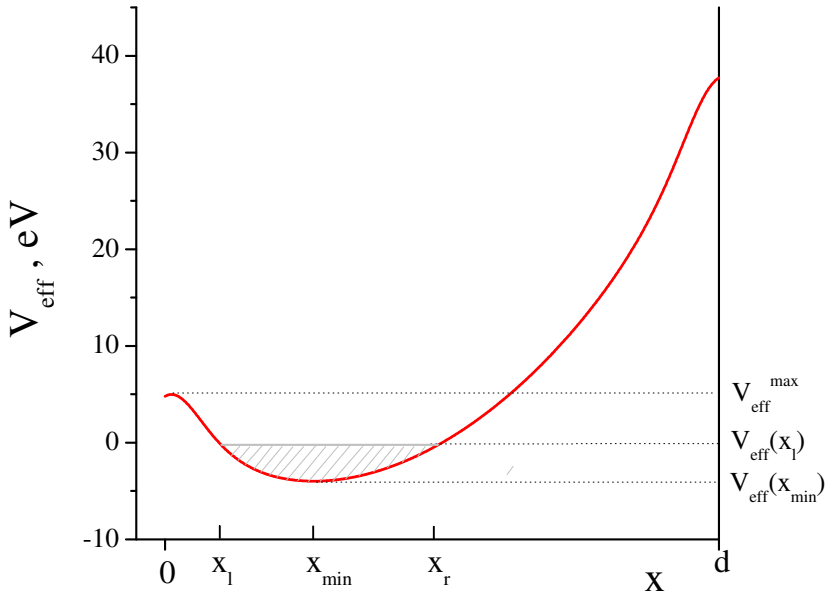

Figure 1. Dependence of the effective potential of bent crystal planes on the distance x from the atomic plane at the bending radius R = 3.5 R_{cr}, x_r and x_l are the coordinates of the right and left reflection points of the channeled positron, x_{min} is the coordinate of the local effective potential minimum, $V_{eff}(x_{min})$ and $V_{eff}^{\max}$ are the local minimal and maximum values of the effective potential inside the given inter-planar interval and $V_{eff}(x_l)$ is the potential value at the boundaries $x_l = x_d$ and x_r of the hatched region of stable channeling motion.

$\varepsilon v_x^2(x)/2 + V_{eff}(x)$ variation, where ε and v_x are the particle total energy and transverse velocity, respectively. However, since the planar potential is close to the harmonic one far from the planes, $\varepsilon_\perp$ will not deviate considerably from its initial value $\varepsilon_{\perp 0} = \varepsilon v_{x0}^2/2 + V_{eff}(x_0)$ for a stably channeled positron. We will also rely on the fact that $\varepsilon_\perp$ will periodically return to the close values with the CU period λ_U in any realistic potential when λ_U substantially exceeds the channeling period λ_{ch} and the adiabatic condition holds true.

Let us remind that channeling is possible in a bent crystal only when its bending radius exceeds the critical value

$$R_{cr} \approx \varepsilon / e E_{\max}, \tag{4}$$

where $E_{\max}$ is the maximal strength of planar electric field, close to $6 \cdot 10^9$ V/cm for Si(110). In general the ratio

$$r = \frac{R_{min}}{R_{cr}} = \frac{E_{max}}{E_{eff}} \tag{5}$$

determines both the depth and the width of the V_{eff} channeling well (see Fig. 1), which, in their turn, limit both the dechanneling length and channeling efficiency (percentage of channeling particles). Below we will find out that the ratio (5) also determines the effective amplitude E_{eff} of the CU field.

To find the optimal value of the ratio (5), we will consider zero incidence case $\vartheta_{x0} = 0$ and assume that stably channeling positrons should not approach the locations of the nuclei closer than by a "dechanneling distance" $x_d \approx 0.02nm$. For this the incidence point coordinate x_0 should belong to the interval $[x_d, x_r]$, where x_r is the right reflection point of the channeling positron having the left one $x_l = x_d$. At this the channeling capture probability will be limited by the value $P_{ch} = (x_r - x_l)/d$ also determined by the ratio (5).

Perhaps the main difference of crystal undulators from the "normal" magnetic one consists in the fast channeling oscillations superimposed on the less frequent undulator ones. The amplitude of the velocity oscillations v_{x0} is related

with the transverse energy by the formulae [1]

$$\varepsilon_{\perp} = \varepsilon v_{x0}^2/2. \tag{6}$$

An initial value $\varepsilon_{\perp 0}$ of the latter is determined by both the coordinate and angle of positron incidence, while its further evolution is caused by the effective crystal potential V_{eff} oscillations induced by that of the local crystal curvature as well as by the incoherent positron scattering by crystal nuclei and electrons. The point is that in practise the maximal value $\varepsilon_{\perp}^{max}$ of (6), measured from the local V_{eff} minimum, can not be reduced with the depth of the potential well by the transition $R_{min} \to R_{cr}$ since both P_{ch} and dechanneling length would nullify therewith. On the other hand, the undulator parameter or a normalized amplitude of the CU velocity oscillations

$$K = Ak_z\gamma = \frac{eE_{eff}\lambda_U}{2\pi\, m} = \frac{eE_{\max}}{2\pi m}\lambda_U\frac{R_{cr}}{R_{\min}} \approx 0.031\lambda_U(\mu m)E_{eff}\left(\frac{GV}{cm}\right) \tag{7}$$

increases with $R_{min} \to R_{cr}$. Thus, the balance of number of channeling positrons, proportional to their capture probability P_{ch} into the channeling regime, of the radiation intensity, proportional to K^2 at small K, and of the dechanneling length, proportional to $\varepsilon_{\perp}^{max}$, has to determine the optimal ratio (5) by maximizing the product

$$F_{opt}(r) = K^2\varepsilon_{\perp}^{max}P_{ch}. \tag{8}$$

The harmonic potential model readily allows one to find the minimizing value $r_{opt}^{harm} = 2.5$, or $R_{min} = 2.5R_{cr}$ analytically. More reliable results of the numerical evaluation of the optimization function (8) in a realistic Moliere potential

[1] the $c = \hbar = 1$ system of units is used.

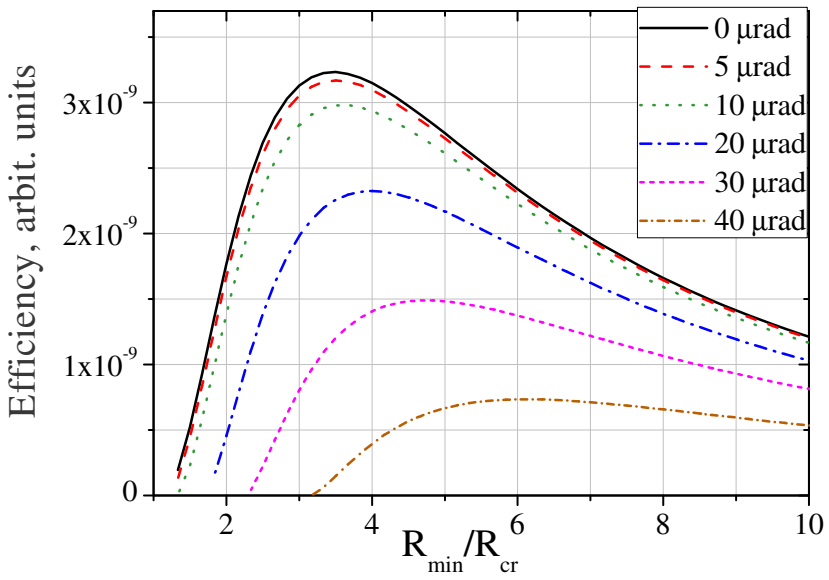

Figure 2. Optimization function (8) dependence on the radii ratio (5) for indicated angles of positron incidence.

are represented in Fig. 2 demonstrating that the optimal value of the ratio (5) increases from $r \simeq 3.5-4$ for the smallest positron beam angular divergencies to $r > 5$ for the larger ones. This circumstance will help us to choose the benchmark CU configuration in Section 4.

For an undulator, or any other periodic structure for coherent radiation production, having a finite number N of periods, the radiation intensity (or probability) is proportional to the square of the interference factor [12,13,14]

$$F_N = \frac{\sin^2(N\Phi/2)}{\sin^2(\Phi/2)}, \tag{9}$$

where

$$\Phi \approx \omega\lambda_U[\theta^2 + (1+K^2)/\gamma^2 + \varepsilon_\perp/\varepsilon]/2 \tag{10}$$

is a relative phase of the waves emitted from neighboring undulator periods at an angle θ with respect to the CU axis by a particle having a transverse energy $\varepsilon_\perp$. Analysing the behavior of the interference factor in the usual way [12,13,14], one can represent the central emission line frequency of the first harmonic of radiation in the forward direction (at $\theta = 0$) in the form

$$\omega_1 = \frac{\gamma^2}{1 + K^2/2 + \varepsilon_{\perp 0}\,\varepsilon/m^2}\frac{2\pi}{\lambda_U}, \tag{11}$$

where $\varepsilon_{\perp 0}$ is some effective average transverse energy, determined by the $\varepsilon_\perp$ distribution both in the channel and along the crystal length. The further analysis of Eqs. (9)-(11) allows one to obtain the contributions by the limited number of CU periods

$$\frac{\delta\omega_N}{\omega_1} = \frac{1}{N} \propto \frac{\lambda_U}{l_{dech}} \propto 1/\sqrt{\varepsilon}, \tag{12}$$

by the radiation collimation angle

$$\frac{\delta\omega_{\,\theta}}{\omega_1} = \frac{\theta^2\gamma^2}{1 + K^2/2 + \varepsilon_{\perp 0}\,\varepsilon/m^2} \tag{13}$$

and by the transverse energy dispersion $\Delta\varepsilon_{\perp max} = \varepsilon_{\perp max} - \varepsilon_{\perp min} = \varepsilon_{\perp max}$

$$\frac{\delta\omega_{\,\varepsilon_\perp}}{\omega_1} = \frac{\Delta\varepsilon_{\perp\,max}\,\varepsilon/m^2}{1 + K^2/2 + \varepsilon_{\perp 0}\,\varepsilon/m^2} \propto \varepsilon \tag{14}$$

to the width of the main undulator radiation peak.

Before using Eqs. (12)-(14) to specify further the CU parameters, we initially fix the CU length to be close to that of dechanneling and the CU period to range from three to four channeling periods to assure, on the one hand, an adiabaticity of the channeling motion in the undulator and, on the other, the hardest radiation at the given positron energy. As a result one finds that

$\delta\omega_N/\omega_1 \propto 1/\sqrt{\varepsilon}$ (see Eq. (12)). Assuming that $K \sim 1$ and neglecting the last term in the Eqs. (14) denominator, one can see that $\delta\omega_{\varepsilon_\perp}/\omega_1 \propto \varepsilon$ (see Eq. (14)). The energy dependencies of these estimates indicate that a positron energy exists which minimizes the combined radiation frequency uncertainty. Unfortunately, it is hardly possible to find exactly this energy using only simple analytical estimates (12) – (14), which allow one to limit the optimal positron energy by the relatively wide interval from 1.5 to 4 GeV. In fact, only a joint exhaustive search of the optimal values of positron energy, CU period, modulation amplitude and length can solve this problem. To provide a benchmark for this search we will chose the lowest value $\varepsilon = 1.5GeV$ from the mentioned interval, the value which was not touched in the literature for some time – see [8].

3 Overview and some details of the simulation method

In general the treatment of particle radiation in CUs is much more complex than that in usual magnetic undulators. First of all, one should take into consideration the dependence of radiation formation process on the variation of particle longitudinal velocity proceeding from the channeling oscillations, the amplitude of which changes both from particle to particle and along the trajectory of each particle. Also the radiation of channeled, never channeled, dechanneled and rechanneled paricles, as well as dechanneling and rechanneling processes themselves should be properly accounted for. All these features can be taken into consideration without their individual study if one uses a reliable method of realistic particle trajectory simulations and direct sampling of the accompanying radiation.

Our simulation method is widely tested using experimental data. The reached level of agreement of its predictions with the latter can be understood from the comparison of our predictions with the data [15] obtained in experiments on electron radiation in the $40\mu m$ CU [4], on the radiation accompanying electron multiple volume reflection from the multitude of the planes of a single-piece crystal [5], and on the electron channeling observation in a thin bent crystal [6]. Since the method has been already described in [4,3], we will dwell here only on the incoherent scattering and photon refraction treatment.

To remind the advantages of our approach, let us start from the model [17] which was the first one described the incoherent scattering of particles moving along classical trajectories. Recently it was applied to simulate the crystal assisted collimation [18]. Remind that incoherent scattering process is treated in [17,18] using the common formulae for the r.m.s particle scattering angles on nuclei and electrons to which the local nucleus and electron densities are substituted. In order to make the relative variations of both averaged crystal field strength and scatterer densities small on each simulation step, the latter have to be chosen rather short. However being applied to the short trajectory steps, the formulae for the r.m.s. scattering angles on both nuclei and electrons can return only small values, demonstrating their inability to realistically describe the single particle scattering at the angles exceeding the r.m.s scattering angle within small trajectory steps (the "large" angles) considerably.

Such an approach is internally contradictive since, though the large-angle scattering events are rare, they nevertheless give the main contribution to the r.m.s. angle of scattering within a small trajectory step. No wonder that single scattering proves to be essential for an adequate joint treatment of coherent and incoherent radiation and pair production [19,20,23,22] as well as for the

quantitative description of the volume capture into the channeling regime of both negatively [23,6] and positively [24] charged particles.

Incoherent scattering, in fact, was treated as a single scattering process long ago by M.L. Ter-Mikaelian [19]. However this approach, being polar to [17,18], is too idealized as well. Indeed, when a particle is moving nearly parallel to a plane or axis, its successive collisions with nuclei and electrons become much more frequent, especially in the regions of maximum local nucleus and electron number densities inside atomic planes and strings, tens of times exceeding their average concentrations in a crystal. That is why we claim that the most adequate way [20,23] both to describe analytically and to simulate numerically the Coulomb scattering at the smallest angles, is to treat it as a multiple scattering process as follows.

In order both to follow the CB theory of [19] and to ensure a proper transition to the well fitted GEANT4 [26] simulation results in the case of amorphous medium, we will adopt the parametrization of the singly-charged particle scattering cross-section

$$\frac{d\sigma}{d\Omega} = \frac{Z^2\alpha^2}{p^2\beta^2}\frac{1}{(\vartheta^2+\vartheta_1^2)^2} \tag{15}$$

from the Thomas-Fermi atom theory. Here p (βc) is the momentum (velocity) of the particle,

$$\vartheta_1 = \frac{\hbar}{p\,a_{TF}}\left[1.13+3.76(\alpha Z/\beta)^2\right]^{1/2} \tag{16}$$

is the typical scattering angle at which the nucleus field screening by electrons becomes important and

$$a_{TF} = (9\pi^2/128Z)^{1/3}(\hbar/me^2) = 0.88534\,a_0/Z^{1/3},$$

where a_0 is the Bohr screening radius, is the screening length suggested by the Thomas-Fermi theory.

M.L. Ter-Mikaelian [19] also predicted some suppression of the incoherent scattering by the correlations in particle collisions with crystal atoms. This effect is explained by an effective merging of small-angle correlated deflections accompanying a sequence of peripheral particle collisions with ordered atoms of a crystal plane or axis into a smooth trajectory bending. Since the latter is described by the "continuum potential", the corresponding small-angle particle scattering contribution should be excluded from the incoherent scattering process (see also [25]). Taking into consideration this incoherent scattering suppression by the Debye-Waller factor, the mean square of the particle multiple scattering angle at a unit length, comprised by the events of single scattering at the angles $\vartheta \leq \vartheta_2$, can be represented in the form

$$\begin{aligned} &\langle \vartheta_s^2(z) \rangle / dz = n_N \int_0^{\vartheta_2} \int_0^{2\pi} \tfrac{d\sigma}{d\Omega} [1 - \exp(-p^2\vartheta^2 u_1^2)] d\varphi \vartheta d\vartheta \\ &= 4\pi \tfrac{Z^2\alpha^2}{\varepsilon^2} n_N \times \{ \ln(1+a) + [1 - \exp(-a \cdot b)]/(1+a) \\ &+ (1+b)\exp(b)\left[E_1(b(1+a)) - E_1(b]\right\}, \end{aligned} \tag{17}$$

were

$$E_1(x) = \int_x^\infty e^{-t} dt/t, \qquad a = \vartheta_2^2/\vartheta_1^2, \quad and \quad b = p^2\vartheta^2 u_1^2.$$

The mean squared multiple scattering angle (17) should be used to sample a cumulative small-angle scattering deflection in both transverse planes using the corresponding 2D Gaussian distribution and azimuthal symmetry assumption (see, however, [25]). The value ϑ_2 is some boundary angle between the single and multiple scattering regions, the choice of which is discussed below. The "large angle" scattering by $\vartheta > \vartheta_2$, complementary to the process

of multiple scattering, is sampled as single scattering events using the same cross-section (15) at the instants of time when a specially sampled random number exceeds the single-scattering probability integrated along the trajectory from either the previous single scattering event or the particle entrance into the crystal. The suppression of incoherent scattering by the atomic correlations in crystals is still taken into consideration by discarding the scattering events in which specially sampled random numbers do not exceed the value $\exp(-p^2\vartheta^2 u_1^2)$. The maximum single scattering angle ϑ_{max} either can be taken equal to the maximum elastic scattering angle by a nucleus or restricted by geometrical and statistical considerations.

The disclosed approach evidently reduces to the model [17] at $\vartheta_2 = \vartheta_{max}$ and to the model [19] at $\vartheta_2 = 0$. Though the latter describes the situation more adequately, it requires more extensive simulations. Our point is that some freedom of the boundary angle ϑ_2 choice exists which allows one to facilitate the simulation procedure. Indeed, the separation of the single-atom scattering angles on "small" and "large", divided by the boundary value ϑ_2, closely reminds that of impact parameters or atom excitation energies in the Bohr-Bethe-Bloch theory of ionization losses. The boundary parameters of the latter enter the logarithms of the intermediate complementary formulae in such a way that they drop out from the resulting formula for ionization losses and, therefore, can be roughly estimated from the qualitative considerations. Similarly one can expect for the weak dependence of the scattering simulation results on ϑ_2.

To choose the latter, let us consider the particle incoherent scattering in the process of its complete deflection by one atomic string or axis, having in mind in particular the positron deflection by a low-index Si plane in the GeV en-

ergy region important for our study of the CU radiation. One can apply the logarithmic approximation to estimate the averaged square of the scattering angle

$$\vartheta_s^2(pl) = 4\pi \frac{Z^2\alpha^2}{\varepsilon^2} \ln(\vartheta_2/\vartheta_1) \int\limits_{pl} n_N dz,$$

where $\int_{pl} n_N dz$ is the integral of nuclei concentration along a half of the positron channeling oscillation, and the incoherent scattering probability

$$P_{sc}(pl) = \frac{\vartheta_s^2(pl)}{\vartheta_2^2 \ln(\vartheta_2/\vartheta_1)}.$$

The latter demonstrates that choosing $\vartheta_2 \sim \vartheta_s(pl)$ one can reduce the probability of positron single Coulomb scattering along the half of the channeling period down to $P_{sc}(pl) \leq 1$ preserving the main features of the incoherent scattering process.

The disclosed method of particle trajectory simulation is applicable to a vast number of processes accompanying high-energy particle motion through crystals. Here we will apply it to the simulation of the spectra of positron radiation in some CU construction. As usual, we will proceed from the formulae

$$\frac{d^2N}{d\omega d\Omega} = \frac{\alpha\omega d\omega}{8\pi^2\varepsilon'^2} \left[\omega^2 |A|^2/\gamma^2 + \left(\varepsilon^2 + \varepsilon'^2\right) |\vec{B}|^2\right] \tag{18}$$

$$A = \int\limits_{-\infty}^{\infty} \exp\{i\varphi(t)\}dt, \quad \vec{B} = \int\limits_{-\infty}^{\infty} \left(\vec{v}_\perp(t) - \vec{\theta}\right) \exp\{i\varphi(t)\}dt, \tag{19}$$

$$\begin{aligned} &\varphi(t) = \omega t - \vec{k}\vec{r} = \int\limits_0^t \dot{\varphi}(t')\, dt' = \tfrac{\omega'}{2} \int\limits_0^t \left[\gamma^{-2} + \omega_p^2/\omega^2 + (\vec{v}_\perp(t') - \vec{\theta})^2\right] dt', \\ &\omega' = \tfrac{\omega\varepsilon}{\varepsilon'}, \end{aligned} \tag{20}$$

derived by the semiclassical operator method by Baier and Katkov [27]. Note that a thorough description of the gamma-photon refraction has been imple-

mented in (18)-(20) by the introduction of the "plasma" refractive index

$$n = k/\omega = 1 - \omega_{pl}^2/2\omega^2. \tag{21}$$

Remind that the photon refraction influence on both channeling and CU radiation is known since the predictions of these effects [28,1,29]. Its importance for CU radiation became even more clear recently. Indeed, the experiments [15,16] on electron radiation in the $40\mu m$ CU have demonstrated some evidence of a peak at photon energies $20 - 60$ keV which are much softer than that of the expected first CU peak. However, to judge, whether such a feature in so soft spectral regio represents itself some new resonant effect, one should first describe the influence of transition radiation from the target surfaces taking into consideration the difference in the thicknesses of the CU crystal and the amorphous target used to measure the radiation background.

The gamma refraction is also essential for another family of CU constructions. Namely, a group of technologies [4] using periodic micro scratches, grooves [30] or thin strips applied to the crystal surface for production of the periodic surface strain can be readily applied to the fabrication of CUs with periods $\lambda_U \sim 1mm$. The point is that even at such high positron energies as 15 GeV, the CU radiation peak frequency (11) practically coincides with the typical energy $\gamma\omega_{pl} \simeq 1MeV$ at which both the density effect and transition radiation are most important.

Another improvement of the method [4] concerns the description of the contributions of the sharp incoherent and smooth coherent deflections into the radiation process. Our recent practice [3,4] suggests to integrate (19) by parts over some trajectory intervals to separate the contributions of sharp and smooth

particle deflection. First – as the contributions of the integration interval ends and second – as the elementary integrals over the intervals analytically evaluated using the uniform field approximation to assure a correct high-frequency behavior without the interval length reduction despite the coherent length decrease. Either the trajectory simulation steps or the larger trajectory parts obtained by the integration steps aggregation can be used as the trajectory intervals. The disclosed approach allows one to represent the integrals (19) in the form

$$A = \int\limits_{-\infty}^{\infty} \exp\{i\varphi(t)\}dt = \tfrac{i}{\dot\varphi(+0)} - \tfrac{i}{\dot\varphi(-0)} +$$
$$i\sum_{i=1}^{N}\left\{\left[\tfrac{1}{\dot\varphi(t_i+0)} - \tfrac{1}{\dot\varphi(t_i-0)}\right]\exp i\varphi(t_i) - \tfrac{2\ddot\varphi(\bar t_i)}{\dot\varphi^3(\bar t_i)}\sin\left[\tfrac{\varphi(t_i-0)-\varphi(t_{i-1}+0)}{2}\right]\exp i\varphi(\bar t_i)\right\},$$

$$\vec B = \int\limits_{-\infty}^{\infty}\left[\vec v_\perp(t) - \vec\theta\right]\exp\{i\varphi(t)\}dt = \left[\tfrac{i}{\dot\varphi(+0)} - \tfrac{i}{\dot\varphi(-0)}\right]\left(\vec v_\perp(0) - \vec\theta\right) +$$
$$i\sum_{i=1}^{N}\left\{\begin{array}{l}\left[\tfrac{\vec v_\perp(t_i)+\vec\vartheta_i-\vec\theta}{\dot\varphi(t_i+0)} - \tfrac{\vec v_\perp(t_i)-\vec\theta}{\dot\varphi(t_i-0)}\right]\exp i\varphi(t_i) - \\ \tfrac{2}{\dot\varphi^2(\bar t_i)}\left[\dot{\vec v}_\perp(\bar t_i) - \left(\vec v_\perp(\bar t_i) - \vec\theta\right)\tfrac{\ddot\varphi(\bar t_i)}{\dot\varphi(\bar t_i)}\right]\sin\left[\tfrac{\varphi(t_i-0)-\varphi(t_{i-1}+0)}{2}\right]\exp i\varphi(\bar t_i)\end{array}\right\}, \quad (22)$$

where $\omega' = \varepsilon/(\varepsilon-\omega)$, $\ddot\varphi(t) = \omega'\left(\vec v_\perp(t_i) - \vec\theta\right)\dot{\vec v}_\perp(t)$, $\bar t_i = (t_i + t_{i-1})/2$, and the derivatives of the phase (20) on the left and on the right of the entrance crystal surface

$$\dot\varphi(-0) = \frac{\omega'}{2}\left[\gamma^{-2} + \left(\vec v_\perp(0) - \vec\theta\right)^2\right],$$
$$\dot\varphi(+0) = \frac{\omega'}{2}\left[\gamma^{-2} + \omega_p^2/\omega^2 + \left(\vec v_\perp(0) - \vec\theta\right)^2\right];$$

on the left and on the right of each inter-step border

$$\dot\varphi(t_i - 0) = \frac{\omega'}{2}\left[\gamma^{-2} + \omega_p^2/\omega^2 + \left(\vec v_\perp(t_i) - \vec\theta\right)^2\right],$$

$$\dot{\varphi}(t_i+0)=\frac{\omega'}{2}\left[\gamma^{-2}+\omega_p^2/\omega^2+\left(\vec{v}_\perp(t_i)+\vec{\vartheta}_i-\vec{\theta}\right)^2\right]$$

and on the right from the exit surface

$$\dot{\varphi}(t_N+0)=\frac{\omega'}{2}\left[\gamma^{-2}+\left(\vec{v}_\perp(T)+\vec{\vartheta}_N-\vec{\theta}\right)^2\right].$$

have been used. We assume here that a particle intersects a plane crystal from the left to the right. The introduced phase derivative breaks at the crystal surfaces and at the trajectory step boundaries allow to treat transition and incoherent radiation, respectively.

Any available experiment, in that number the ones [15,16,9] on the electron CU radiation, should be used both to verify the simulation tool and to demonstrate the scope of its applicability. The outcomes of the experiment [15] with 855 MeV electrons have been already reproduced in [4]. Both the modest radiation spectrum modification at the expected CU peak position and the channeling radiation suppression in the CU have been reproduced. Provided the information on the real CU parameters, a quantitative reproduction of this experiment will be readily given. The same is true for the analogous experiments with 270 MeV [15] and 375 MeV [16] electrons in the same CU.

Here we reproduce the recent experimental results [9] obtained with the short-period small-amplitude CU suggested by A. Kostyuk [10]. From Fig. 3 one can conclude that the short period small amplitude crystal plane modulation induces the radiation spectrum modification near 15 MeV by about 10% of the height of the channeling radiation maximum at 5 MeV. More strict reproduction of the experiment [9] is hampered by the insufficient information on the actual parameters of both the undulator and the electron angular distribution.

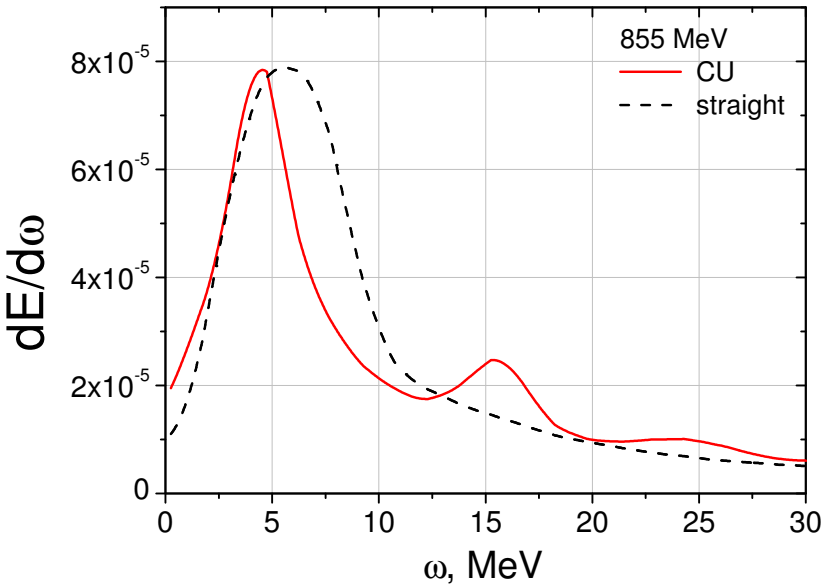

Figure 3. Spectral distribution of 855 MeV electron radiation in a short-period CU with $\lambda_U = 4.3\mu m$, $A = 0.013nm$ and length of $3\mu m$ (solid) and in a plane $Si(110)$ crystal of the same length. Electron beam divergence equals $176\mu rad$.

The detail simulations of the electron channeling in both [4] and [6] reveales a drastic instability of the electron channeling in CUs stimulating one to rely more on the positron ones. Proceeding to the simulations of the latter, we present the results of simulations of the positron channeling experiment [11] in Fig. 4. Here again the reaching of the better agreement of simulations with the experiment is hampered by an incomplete information on the angular characteristics of both the positron and gamma-photon beams.

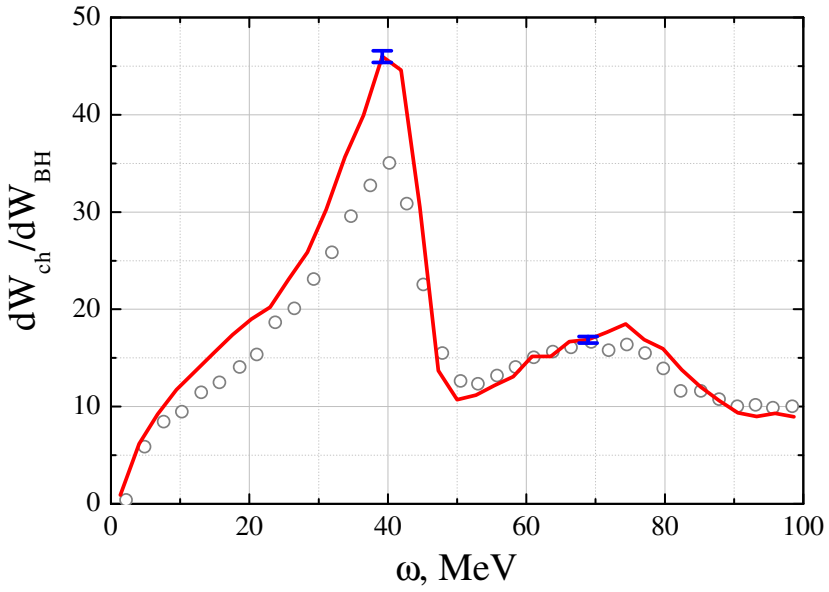

Figure 4. Enhancement factor over the Bethe-Heitler radiation intensity by that of the 6.7 GeV positrons channeling in a 105 μm thick Si (110) crystal. The incidence angles are $-\theta_{ch} < \theta_{ex} < \theta_{ch},\ \theta_{ch} < \theta_{ey} < \theta_{ch}$, where $\theta_{ch} = 62\mu rad$. The collimation angles are $-\theta_{coll} < \theta_{\gamma x} < \theta_{coll},\ -\theta_{coll} < \theta_{\gamma y} < \theta_{coll}$, where $\theta_{coll} = 350\mu rad$. Open circles represent experimental data from [11]. The bars represent statistical simulation errors.

4 Simulation of a CU functioning

Some additional assumptions are necessary to apply eqs. (5), (7) and (12)-(14) to fix the parameters of the benchmark CU assuring the lowest spectral width. First we will choose the CU length to be slightly less than the positron dechennling length. Also we will follow the traditional understanding of the CU functioning, in which the positron channeling in CU can be treated adiabatically, assuming $\lambda_U = (3 \div 4)\lambda_{ch}$. The choice of practically the minimal λ_U value, assuring adiabatical condition, provides both the shortest undulator radiation wavelength, minimal undulator length and positron energy as well

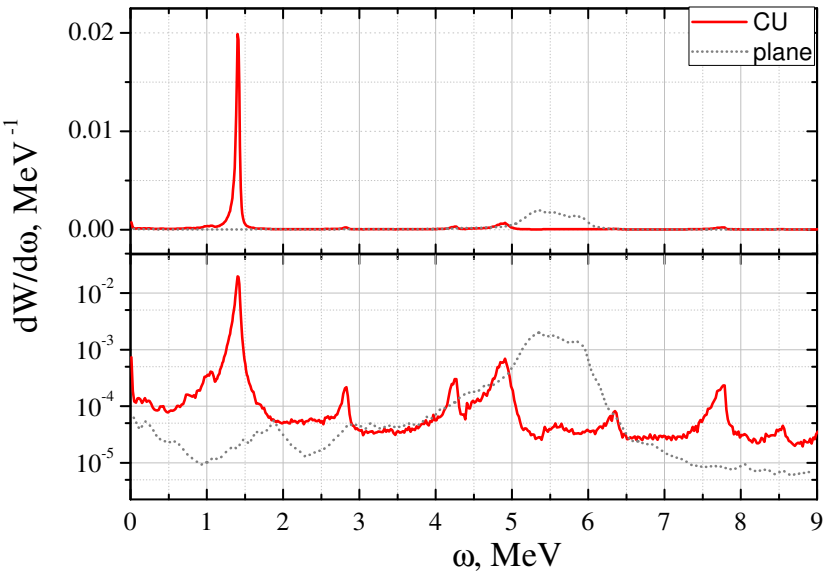

Figure 5. Spectral distribution of the radiation emitted by a 1.5 GeV positron in the linear (top) and logarithmic (bottom) scale: solid line – in the Si (110) CU (24) and dotted line – in a plane 0.48 mm Si (110) crystal. Positron beam incidence angle equals zero, its angular divergence is $\Delta\theta_e = 10\mu rad$ and collimation semi-apex angle is $\Delta\theta_\gamma = 1/8\gamma = 42.6\mu rad$.

as softens the requirements on the positron beam angular divergence. Finding then a minimum of either the sum of the widths Eqs. (12) and (14) or of their squares and taking into consideration the numerous uncertainties of all the assumptions made, one can both restrict the "optimal" positron energy interval $\varepsilon = (1.5 \div 4)GeV$ and fix the minimum radiation spectrum width

$$\Delta\omega/\omega \simeq 3\%. \tag{23}$$

Finding these estimates we have also assumed the $K \sim 1$ and $R_{min} = 3.5R_{cr}$. We chose the minimal positron energy from the found interval which jointly with both the previous assumptions and Eqs. (5), (7), (12)-(14) fixes the pa-

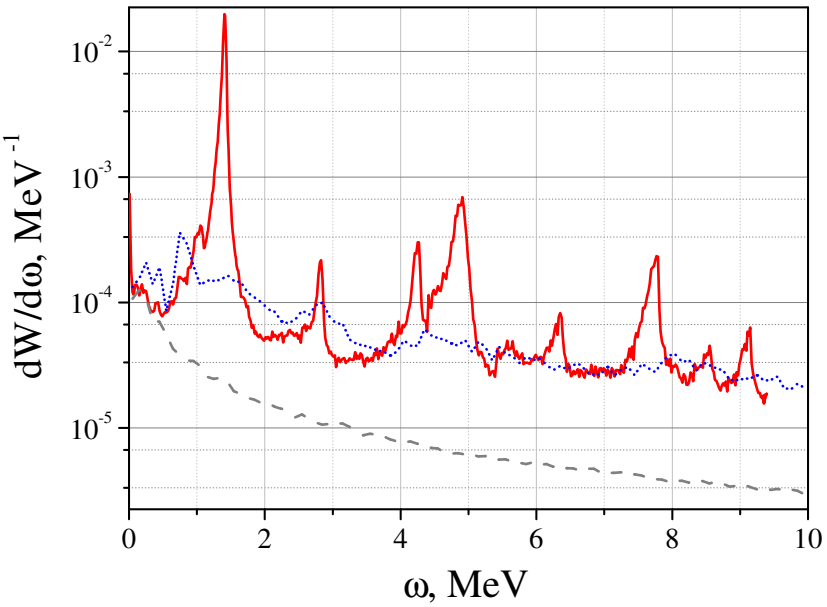

Figure 6. Spectral distribution of the radiation: solid line – emitted by the all positrons in the CU (24), dotted line – by only the initially nonchanneled positrons in the same CU and dashed line – by all the positrons in a 0.48 mm amorphous Si plate. Positron energy equals 1.5 GeV. All the probabilities are normalized on one positron.

rameters

$$\varepsilon = 1.5\,GeV, \quad \lambda_U = 12\,\mu m, \quad A = 0.4\,nm, \quad L_U = 40\lambda_U = 0.48\,mm \tag{24}$$

of the CU scheme we would like to suggest here as a benchmark for further investigations. It should be mentioned that $K = 0.64$ in this construction. The results of the simulations of positron motion and radiation in the CU (24) are illustrated in Figs. 5-8 which confirm the main prediction (23) concerning the CU radiation spectrum width $\Delta\omega/\omega \simeq 0.05/1.4 \simeq 3.5\%$ and enlighten some other some important details.

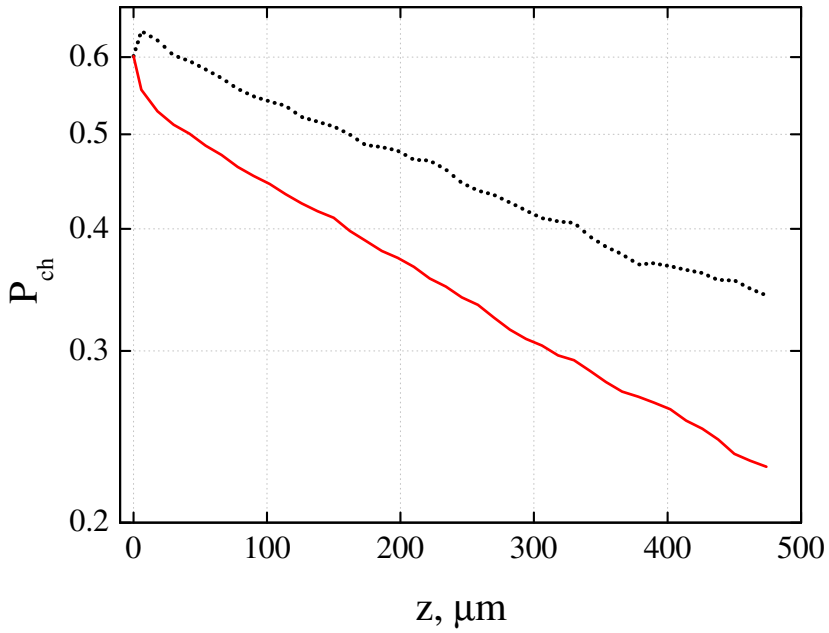

Figure 7. 1.5 GeV positron channeling probability dependence on crystal depth with (dotted, $l_{dch} = 0.8$ mm) and without (solid line, $l_{dch} = 0.56$ mm) rechanneling consideration for the same CU.

This way Fig. 5 illustrates a great suppression of the channeling radiation in the CU, primarily explained by both oscillation amplitude reduction of the positrons stably channeling in CU and moving them off the regions of the strongest planar field for a considerable part of the CU period. Some frequency decrease of the channeling radiation in the CU is readily explained by the joint effect of the radiation collimation and variations of local plane orientation in CU.

Fig. 6 demonstrates that the peak spectral intensity of radiation of positrons channeling in the CU exceeds that of the comparable number of nonchanneled ones by two orders of value and that in the amorphous Si target of the same thickness – by nearly three orders of value.

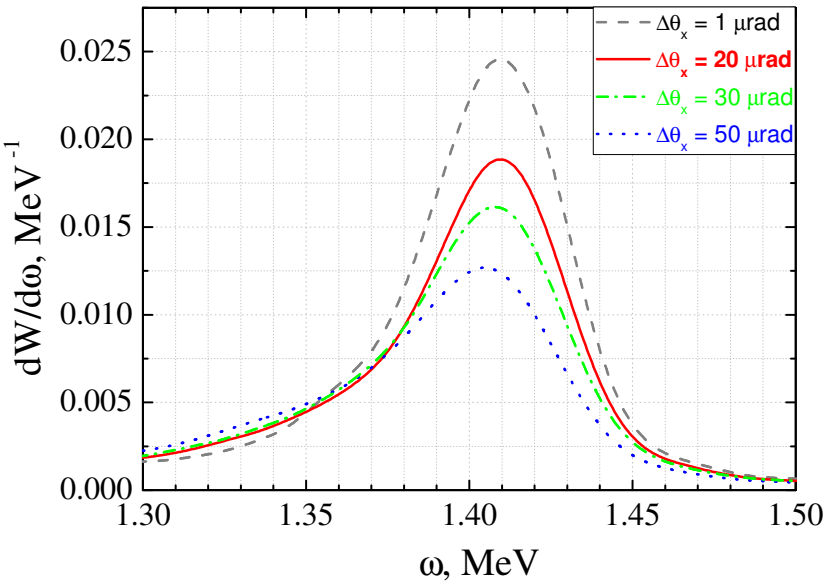

Figure 8. Spectral distribution of the radiation emitted in the main peak region in the same CU at the indicated values of r.m.s Gaussian positron beam divergences.

Fig. 7 both confirms our assumption concerning the value of positron dechanneling length and illustrates an importance of the positron rechanneling, the effect recently observed for electrons [4,6].

Fig. 8 illustrates the role of incident beam divergence demonstrating that the positron collimation requirements are quite severe. The same is true for the emitted radiation. In order to prevent a considerable spectral widening caused by the radiation angular divergence we used the condition (13) to restrict the collimation angle to $\theta_{coll} = 1/8\gamma \simeq 43\mu rad$. Such a low value results in a rather low gamma-photon yield of about $0.001\gamma/e^+$ which, however, can be increased, at least several times at a prise of a moderate spectrum widening by the two-three time increase of the collimation angle.

5 Conclusions

Relying on the original estimates of both the CU radiation intensity and various contributions to the radiation spectrum width a construction of positron CU, characterized by 3.5 – 4% spectrum line width, $10^{-3}\gamma/e^+$ photon yield, an order of value channeling radiation suppression and severe requirements on both gamma and positron beam collimation is devised. We suggest to consider this CU configuration as a benchmark for both estimates of CU application perspectives and further development of effective CU constructions.

The author is grateful to Prof. Baryshevsky and Dr. Maisheev for useful discussions and to Prof. Guidi and his group for a continuous collaboration.

References

[1] V.G. Baryshevsky, I.Ya.Dubovskaya, and A.O. Grubich, Phys. Lett. **77A**(1980)61.

[2] V.V. Kaplin, S.V. Plotnikov and S.A. Vorobijev, Zh.Tech. Fiz. **50**(1980)1079 [English translation: Sov. Phys.-Tech Phys. **25**(1980)650].

[3] V. Guidi, L. Bandiera and V.V. Tikhomirov, Phys. Rev. A **86**(2012) 042903(11pp).

[4] V.G. Baryshevsky, V.V. Tikhomirov, Nucl. Instrum. And Methods. B **309**(2013) 30.

[5] L. Bandiera et al., Phys. Rev. Lett. **111** (2013) 255502.

[6] A. Mazzolari et al., Phys. Rev. Lett. **112** (2014) 135503.

[7] S. Bellucci, V.A. Maisheev, J. Phys.: Condens. Matter **18** (2006) S2083S2093.

[8] A.V. Korol, A.V. Solov'yov and W. Greiner. Channeling and Radiation in Periodically Bent Crystals (Springer Series on Atomic, Optical and Plasma Physics 69).

[9] T. N. Wistisen et al., Phys. Rev. Lett. **112** (2014) 254801.

[10] A. Kostyuk, Phys. Rev. Lett. **110** (2013) 15503.

[11] J. Bak et al., Nucl.Phys. **B254**(1985)491.

[12] P. Elleaume, Beam Line 2002 **32** 1. P. 14.

[13] M.M. Nikitin, V. Ya. Epp, Undulator radiation. Moscow. Energoizdat, 1988. (in Russian).

[14] R. Rullhusen, X. Artru, and P. Dhez, Novel radiation sources using relativistic electrons. From infrared to x-rays. World Scientific Publishing Co. Pte. Ltd., 1998.

[15] H. Backe et al., Nucl. Instrum. Methods Phys. Res. **309**(2013)37.

[16] H. Backe et al., J. Phys. Conf. Ser. **438**(2013)012017.

[17] A.M. Taratin and S. A. Vorobiev, Sov. Phys. Tech. Phys. **30**(1985)927.

[18] W. Scandale and A. Taratin, Simulation of "CRYSTAL", the bent crystal based collimation experiment in the SPS, CERN/AT 2008-21.

[19] M. L. Ter-Mikaelian, High-energy electromagnetic processes in condensed media. Wiley. New York, 1972.

[20] V. G. Baryshevskii, V. V. Tikhomirov, Sov. Phys. JETP. **63**(1986)1116.

[21] V. V. Tikhomirov, J. Physique. (Paris). **48**(1987)1009.

[22] X. Artru, Nucl. Instr. Meth. in Phys. Res. B **48**(1990)278.

[23] V. V. Tikhomirov, Nucl. Instr. Meth. in Phys. Res. B **36**(1989)282.

[24] V.M.Biryukov, Y.A.Chesnokov, V.I.Kotov, Crystal Channeling and Its Application at High-Energy Accelerators, Springer-Verlag, 1997, 219 p.

[25] V.L. Lyuboshitz, M.I. Podgoretskii, Sov. Phys. JETP. **60**(1984)409

[26] http://geant4.cern.ch/ JEANT4 4 9.5.0 Physics Reference Manual (6.70) - (6.73).

[27] V. N. Baier, V.M. Katkov, and V. M. Strakhovenko, Electromagnetic Processes at High Energies in Oriented Single Crystals (World Scientific, Singapore, 1998).

[28] V. G. Baryshevskii and I. Ya. Dubovskaya, Phys. Status Solidi (b) **82**(1977)403.

[29] V. G. Baryshevskii and I. Ya. Dubovskaya, J. Phys.: Condensed Matter **3**(14)(1991)2421.

[30] E. Bagli et. al. Eur. Phys. J. C **74**(2014)3114.